Soil Environ. 45(1): 109-126, 2026
DOI: doi.org/10.25252/SE/2026/253992
Online ISSN: 2075-1141
Print ISSN: 2074-9546

Improving soil health and tomato production in a reduced nitrogen system: The role of biochar and organic fertilizer coupling

Zihan Yue[1], Di Tian[1], Liyan Dong[2] and Weihua Wang[1*]
[1]Faculty of Modern Agricultural Engineering, Kunming University of Science and Technology, Kunming 650500, China
[2]Panzhihua Academy of Agriculture and Forestry Sciences, Panzhihua 617000, China
***[Received:** December 07, 2025 **Accepted:** January 17, 2026 **Published Online:** February 07, 2026]*

Abstract

Conventional nitrogen fertilization frequently results in soil degradation and environmental pollution. While the isolated effects of nitrogen reduction, organic amendments, or biochar have been explored, their synergistic interactions remain inadequately understood. This two-year field study in Yunnan, China, addressed this gap by evaluating the coupling effects of biochar (applied at 10, 15, and 20 t ha^{-1}) with three organic fertilizers (chicken manure, cattle manure, and earthworm castings) under a consistent 40% nitrogen reduction. The primary objective was to establish a technical pathway for synergistic fertilizer reduction, waste utilization, and sustainable soil management. Results demonstrated that the combination of earthworm castings and biochar (15 t ha^{-1}), designated as treatment F3B2, most significantly enhanced soil nutrient supply and microbial diversity. This treatment yielded the highest relative abundance of the top 10 bacterial genera and maximum bacterial Chao1 indices of 3028.06 and 3087.18 in the first and second years, representing increases of 10.13% and 18.50% compared to the control (CK), respectively. Agronomically, the F3B2 treatment increased tomato yield by 23.75% and vitamin C content by 14.65% in the second year. Furthermore, TOPSIS analysis consistently ranked F3B2 as the optimal integrated management strategy. This study provides a replicable paradigm for green and efficient production in protected vegetable cultivation systems. In conclusion, the integrated application of organic fertilizer and biochar under reduced nitrogen conditions synergistically optimizes soil health—particularly by enhancing the microbial community—and significantly promotes tomato growth, yield, and quality.

Keywords: Biochar; Organic fertilizer; Nitrogen reduction; Soil health; Rhizosphere microbiome; Sustainable agriculture

Introduction

Globally, agriculture stands at a crossroads, facing a dual challenge: increasing productivity to feed a growing population while reducing its environmental footprint to combat climate change (Rockström *et al.*, 2020). Over the past half-century, excessive reliance on synthetic fertilizers has pushed nitrogen and phosphorus cycles beyond safe operating spaces, leading to widespread soil degradation and biodiversity loss (Richardson *et al.*, 2023). Soil health is the cornerstone of productive and sustainable agricultural ecosystems (Lehmann *et al.*, 2020). However, inappropriate fertilization practices often lead to soil nutrient imbalances, undermining soil health and crop productivity. This not only threatens agricultural stability but also jeopardizes the long-term sustainability of farming systems, posing significant risks to agricultural safety and development (Saha *et al.*, 2024). Tomato, as a vital economic crop, frequently faces multiple challenges under conventional fertilization: soil acidification due to nutrient imbalance (Tao *et al.*, 2019), insufficient nitrogen use efficiency leading to nitrogen and phosphorus leaching and elevated nitrate risks in groundwater (Alam *et al.*, 2024), and intensified soil degradation accompanied by an increased prevalence of soil-borne diseases (Wang *et al.*, 2022).

In this context, the integration of organic fertilizers and biochar emerges as a promising solution (Bai *et al.*, 2022). Organic fertilizers, rich in organic matter and diverse nutrients, are highly effective in improving soil structure, stimulating the growth and activity of beneficial soil microorganisms, and consequently enhancing soil fertility and ecological functions. Meanwhile, biochar, with its distinctive porous structure and high stability, plays a significant role in modifying soil physico-chemical

***Email:** wangweihua1220@163.com
Cite This Paper: Yue, Z., D. Tian, L. Dong and W. Wang. 2026. Improving soil health and tomato production in a reduced nitrogen system: The role of biochar and organic fertilizer coupling. *Soil Environ*. 45(1): 109-126.

properties, immobilizing pollutants, and sequestering carbon to reduce emissions (Hu *et al.*, 2024). The combined application of these amendments, particularly under reduced nitrogen conditions, is hypothesized to synergistically improve the tomato rhizosphere microecology, enhance nutrient availability and microbial diversity, decrease dependence on nitrogen fertilizers, and collectively promote tomato growth, yield, and fruit quality.

Substantial research has explored the agricultural application of organic fertilizers and biochar. For instance, Hu and colleagues (2023), through an extensive eight-year field trial, found that the co-application of biochar and organic fertilizer, compared to mineral fertilizer alone, significantly increased soil available phosphorus, reduced stable phosphorus, stimulated soil phosphatase activity, and enriched phosphorus-solubilizing genes, thereby enhancing phosphorus uptake and yield in corn. Rivelli and Libutti (2022) demonstrated that biochar, especially when combined with compost, improved soil properties and leaf nutrient content in Swiss chard, effectively boosting yield and quality. Hong and colleagues (2022) showed that a combined amendment of seaweed-based organic fertilizer, apatite, and biochar (at a 2% application rate in a 1:0.5:1.5 ratio) markedly increased soil pH and electrical conductivity, reduced the bioavailability of cadmium, lead, and chromium, enhanced soil organic matter and nutrient levels, improved corn yield and quality, and induced significant shifts in the soil microbial community structure, proving effective for rehabilitating heavy metal-polluted soils.

However, current fertilization research remains fragmented. Most studies focus on isolated factors—either reducing nitrogen or adding a single amendment—rather than evaluating them as an integrated system. This leaves the intricate interactions between chemical fertilizers, organic fertilizers, and biochar largely unexplored, hindering the development of more efficient and sustainable fertilization techniques. Moreover, a systematic assessment of the "soil-crop" system interaction under the integrated scenario of nitrogen reduction, strategic organic fertilization, and biochar amendment remains lacking.

Within the framework of modern agricultural reforms, this study uses tomato as a model crop to fill this knowledge gap. This study systematically analyzes the comprehensive impacts of a coupled model synergizing nitrogen reduction, efficient organic fertilizer utilization, and optimized biochar application on soil structural characteristics, the micro-ecological environment, and tomato yield and quality. This study further explores the mechanisms that support sustainable development of the soil–crop system under reduced nitrogen fertilization. The specific objectives are (1) to investigate the effects of combined organic fertilizer and biochar application under nitrogen reduction on the properties of tomato rhizosphere soil; (2) to elucidate how this combination shapes the micro-ecosystem of the tomato rhizosphere; and (3) to comprehensively evaluate its impact on tomato yield and quality. Ultimately, this research is intended to establish a technical pathway for fertilizer reduction, waste utilization, and sustainable soil management, providing insights relevant for green and efficient production in protected cultivation and broader agricultural ecosystems.

Materials and Methods

Overview of the experimental site

The experimental site is located in Jinning, Yunnan (102°60′ E, 24°72′ N), characterized by a subtropical plateau monsoon climate (Figure 1). The annual average precipitation is approximately 1055.4 mm, with an average annual temperature of about 16.4°C. The highest temperatures occur in June (21.2°C), while the lowest temperatures are recorded in January (9.4°C). Relative humidity is higher during the rainy season, exceeding 79% from August to October, and relatively lower during the dry season, particularly noticeable from February to April (Table 1). The highland red soil used in the experiment has a bulk density of 1.165 g cm^{-3}, with 52.27% sand, 32.65% silt, and 15.08% clay; pH 6.5; organic matter content: 11.21 g kg^{-1}; alkali-hydrolyzable nitrogen: 60.12 mg kg^{-1}; available phosphorus: 32.05 mg kg^{-1}; and available potassium: 110.51 mg kg^{-1}. The soil exhibits characteristics of "good aeration, poor nutrient retention, moderate nitrogen, phosphorus deficiency, and moderate potassium."

Test materials

The test tomatoes were the indeterminate variety "Shanghai Guofen," introduced to Yuanmou, Yunnan. Seedlings were cultivated using floating seedling technology: On February 10, plump, disease-free seeds were sown at a rate of three per cell in a foam tray filled with a mixture of humus soil and perlite (3:1) foam seedling trays and placed in a water-filled seedling pool until the four-leaf stage. Healthy seedlings with uniform growth were selected for transplanting. The biochar used in the experiment was supplied by Yuzhongao Agricultural Technology Co., Ltd. This material was produced from wheat straw through slow pyrolysis at high temperatures (550-600°C) under anoxic conditions for 4-6 hours. Prior to

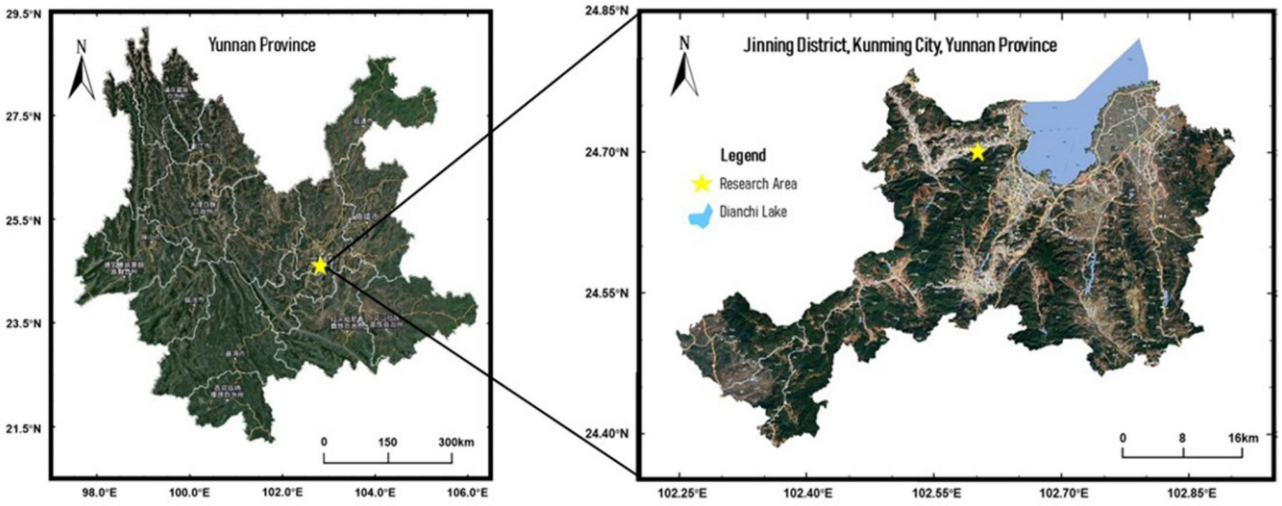

Figure 1: Location of the study area

Table 1: Monthly average precipitation, temperature, and relative humidity data for Jinning, Yunnan Province, from 2014 to 2024

Month	Jan	Feb	Mar	Apr	May	Jun	Jul	Aug	Sep	Oct	Nov	Dec	Mean	Total
Precipitation (mm)	31.0	9.6	18.8	29.6	54.8	190.1	208.4	238.9	158.7	75.9	25.8	14.5	/	1055.4
Temperature (°C)	9.4	11.4	15.6	18.0	20.4	21.2	20.9	20.7	19.4	16.4	13.1	9.9	16.4	/
Relative humidity (%)	66.9	59.3	51.7	54.5	60.1	73.5	77.8	79.2	79.1	79.5	73.6	72.9	69.0	/

Table 2: Basic traits of organic fertilizers for testing

Type	Organic matter g kg^{-1}	Total nitrogen g kg^{-1}	Total phosphorus g kg^{-1}	Total potassium g kg^{-1}	Available nitrogen mg kg^{-1}	Available phosphorus mg kg^{-1}	Available potassium mg kg^{-1}
Chicken manure	206.03	28.01	24.32	21.62	211.33	132.71	208.42
Cow manure	118.31	24.51	19.87	16.51	115.67	98.75	124.51
Earthworm manure	287.16	15.01	31.41	28.17	267.33	187.14	211.34

use, it was ground and sieved through a 0.5 mm mesh. Its fundamental physicochemical properties included strong alkalinity (pH 10.24), high total porosity (67.03%), and cation exchange capacity (30.8 cmol kg^{-1}), with a specific surface area of 9.12 m^2 g^{-1}. Elemental analysis revealed total nitrogen, phosphorus, and potassium contents of 7.25, 3.46, and 6.78 g kg^{-1}, respectively, with ash content at 11.55%. Chemical fertilizers selected were urea (46% N), superphosphate (60% P_2O_5), and potassium sulfate (52% K_2O). Organic fertilizers comprised fermented chicken manure, cattle manure, and earthworm castings (nutrient content shown in Table 2).

Experimental design

The trial commenced in April 2023. Three biochar application rates were established: B1 (10 t hm^{-2}), B2 (15 t hm^{-2}), and B3 (20 t hm^{-2}). × 3 organic fertilizer types (F1 chicken manure, F2 cattle manure, F3 earthworm castings) + control group (CK), totaling 10 treatments. Total nitrogen input was uniformly set at 47.6–48.15 g m^{-2} following the principle of nitrogen-equivalent replacement. Specific application rates for each treatment are detailed in Table 3. Following the "soil testing-formulation-fertilizer application" approach, nutrient requirements were calculated based on target yields of 97,500–112,500 kg ha^{-1}

Table 3: Field trial treatments

Total nitrogen	Treatment	Nitrogenous fertilizer		Organic fertilizer		Biochar	
		Nitrogen content	The amount applied	Nitrogen content	The amount applied	Nitrogen content	The amount applied
47.6~48.15 g m^{-2}	CK	48.01 g m^{-2}	100% (104.3 g m^{-2})	/	/	/	/
	F1B1	28.81 g m^{-2}	60% (62.58 g m^{-2})	11.95 g m^{-2}	Chicken manure (427 g m^{-2})	7.25 g m^{-2}	B1 (10 t hm^{-2})
	F2B1				Cow manure (489 g m^{-2})		
	F3B1				Earthworm manure (796 g m^{-2})		
	F1B2	28.81 g m^{-2}	60% (62.58 g m^{-2})	8.32 g m^{-2}	Chicken manure (297 g m^{-2})	11.01 g m^{-2}	B2 (15 t hm^{-2})
	F2B2				Cow manure (340 g m^{-2})		
	F3B2				Earthworm manure (554 g m^{-2})		
	F1B3	28.81 g m^{-2}	60% (62.58 g m^{-2})	4.70 g m^{-2}	Chicken manure (168 g m^{-2})	14.51 g m^{-2}	B3 (20 t hm^{-2})
	F2B3				Cow manure (192 g m^{-2})		
	F3B3				Earthworm manure (313 g m^{-2})		

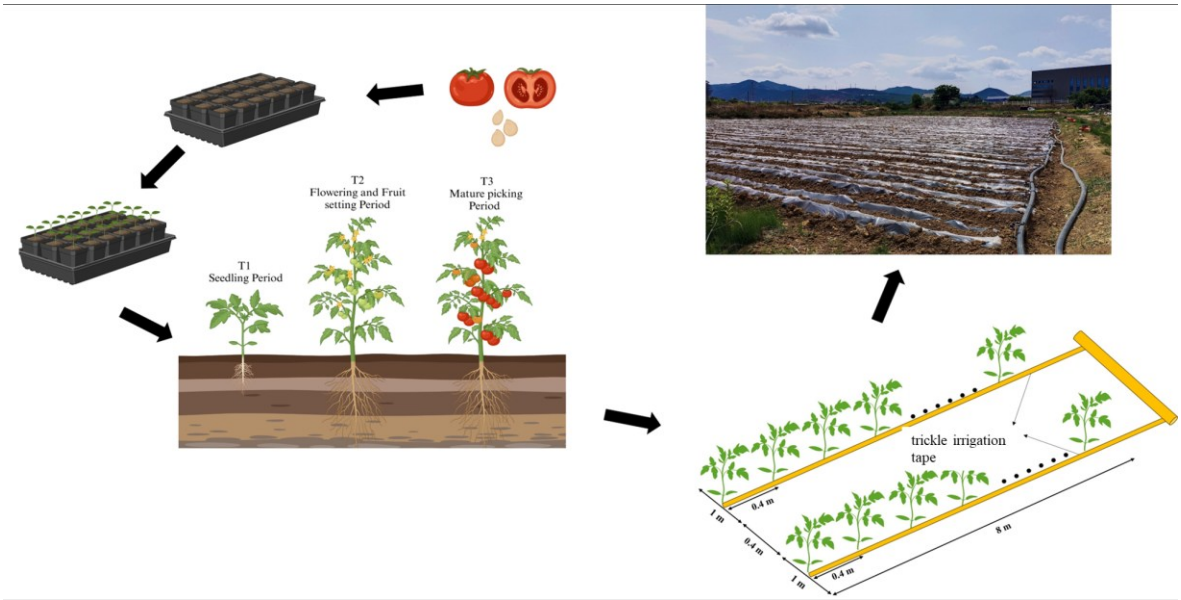

Figure 2: Division of experimental plots and fertility periods

and nutrient needs of N 4.5, P_2O_5 0.92, and K_2O 5.2 kg t^{-1}. The basal fertilizer was applied in a single application on April 11, the day of transplanting, consisting of organic fertilizer + 100% of P + 15% of N and K. The remaining 85% of N and K were applied in three split applications via precision drip irrigation with water-fertilizer integration at the following timepoints: April 26 (after seedling establishment), May 28 (first ear fruit enlargement stage), and June 11 (second and third ear fruit enlargement stages). A randomized block design was employed with 8 m² plots, featuring 1.5 m isolation strips longitudinally and protective ridges transversely. Equal water and fertilizer management was maintained throughout the entire growth period. The specific layout plan of the field plots and the detailed division of growth periods can be referred to in Figure 2. Biochar was applied once, followed by continuous cropping for two years, while basal fertilizer was applied annually.

Sample collection and Measurement methods

Sample collection

Soil sampling for the experiment was conducted at three growth stages: seedling stage (May 11), fruit enlargement stage (July 10), and harvest maturity stage (September 5). During sampling, a portable soil sampler was used to collect soil samples at a depth of 0–20 cm in each experimental plot (with three replicates per treatment) using the serpentine sampling method. Five subsamples were randomly selected from each plot to form a composite sample. All freshly collected soil samples were immediately transferred into sterile polyethylene resealable bags and transported to the laboratory for subsequent processing. The processing workflow included three preservation methods: (1) Air-dried subsamples were ground and sieved for physicochemical property analysis; (2) A portion of fresh soil was stored at 4°C for microbial biomass determination; (3) A third portion was frozen at -80°C for DNA extraction to enable high-throughput microbial community analysis.

Measurement method

Soil water-stable aggregates were analyzed using dry sieving to determine the particle size distribution of mechanically stable aggregates and wet sieving to classify water-stable aggregate sizes. Mechanically stable aggregates were categorized as large aggregates (≥0.25 mm) and micro-aggregates (<0.25 mm), while water-stable aggregates were classified into three tiers based on ecological function (Hu *et al.*, 2020). Aggregate stability characteristics were quantified using mean weight diameter (MWD) and geometric mean diameter (GMD) (Cheng *et al.*, 2023). Soil available phosphorus was extracted with 0.5 M sodium bicarbonate (pH 8.5) and quantified colorimetrically using a molybdenum-antimony reagent (Olsen, 1954). Available potassium was extracted with 1 M neutral ammonium acetate and measured directly by flame photometry (Knudsen *et al.*, 1982). Total nitrogen was determined by the Kjeldahl method, involving digestion with concentrated sulfuric acid and a catalyst, followed by distillation and titration (Bremner & Mulvaney, 1982).

Soil microbial properties were assessed by Yangling Xinhua Sheng Ecology Technology Co., Ltd. using Illumina MiSeq platform sequencing (PE250 strategy) for microbiome analysis. This included soil sample collection, DNA extraction, primer design for PCR amplification, DNA concentration and purity testing, OTU classification and annotation, and diversity index calculation (Di Bella *et al.*, 2013). The specific experimental procedure includes weighing 0.5 g of soil sample, extracting total DNA using the Power Soil DNA extraction kit, and assessing DNA concentration and purity via the NanoDrop ND-1000 spectrophotometer and 1% agarose gel electrophoresis. The DNA is then stored at -20°C. Specific amplification primers were designed for bacterial 16S rRNA genes (primers 515F/907R) and fungal ITS genes (primers ITS1F/ITS2R). Following PCR amplification, PCR products from the same sample were pooled. After preliminary quantification via 2% agarose gel electrophoresis, DNA concentrations were precisely measured using the QuantiFluor™-ST Blue Fluorescence Quantification System. Libraries were then pooled and normalized according to sequencing requirements. Operational Taxonomic Units (OTUs) were further classified based on sequence similarity using QIIME software. OTU representative sequences were annotated for species in the SILVA (v138.1) and UNITE (v8.2) databases (RDP classifier, 97% similarity threshold). Community composition structures were statistically analyzed at the phylum and genus levels. Alpha diversity indices, including Shannon, Simpson, and Chao1 indices, were calculated from OTU data, alongside beta diversity analysis for soil bacteria.

Fruit yield was assessed using dynamic monitoring. Three plants were randomly selected per plot, and data were recorded through staged harvests during the maturation period. Yield was calculated, and significant differences were tested (Akhtar *et al.*, 2014). Tomato quality was evaluated at full maturity by sampling three plants. After pretreatment, soluble total sugars, vitamin C, organic acid content, and soluble solids were measured.

Data processing and Analysis

The experimental data were collected, organized, and subjected to variance analysis ($\alpha = 0.05$) using Excel 2010 and SPSS Statistics 26.0 software. Duncan multiple comparison and Pearson correlation analysis were also conducted.

Topsis analysis

The TOPSIS (Technique for Order Preference by Similarity to the Ideal Solution) is a widely adopted approach for multi-criteria decision-making, which involves ranking options based on their proximity to an optimal benchmark and their distance from the least favorable scenario. The fundamental principle is to assess the merits and drawbacks of each choice by measuring the Euclidean distances from both the best possible (positive ideal) and worst possible (negative ideal) solutions (Miao *et al.*, 2022). The detailed process for applying this method is outlined below:

A decision matrix was developed by compiling the data collected from each indicator during the agricultural experiment. This resulted in an n-by-m matrix, with 'n' representing the number of different treatment options and 'm' denoting the number of evaluation criteria. The rows correspond to various experimental treatments, while the columns detail the specific indicators used for assessment.

The standardization of the data was achieved via the range technique, thus eradicating discrepancies across dimensions and securing uniformity in comparison between diverse measures.

$$x_{ij}^{*} = \frac{x_{ij} - \min(x_j)}{\max(x_j) - \min(x_j)} \quad (2.1)$$

In the formula, x_{ij} is the value of the j-th indicator for the i-th sample.

The positive and negative ideal solutions were determined by obtaining the maximum and minimum values of each indicator as the positive ideal solution A^{+} and the negative ideal solution A^{-}.

The distances from each alternative to the positive and negative ideal solutions were calculated using the Euclidean distance formula.

$$D_i^{+} = \sqrt{\sum_{j=1}^{m} \left(v_{ij} - v_j^{+}\right)^2} \quad (2.2)$$

$$D_i^{-} = \sqrt{\sum_{j=1}^{m} \left(v_{ij} - v_j^{-}\right)^2} \quad (2.3)$$

The relative closeness was calculated for each experimental treatment C_i:

$$C_i = \frac{D_i^{-}}{D_i^{+} + D_i^{-}} \quad (2.4)$$

The value range is between 0 and 1. The closer C_i is to 1, the better the comprehensive evaluation under that treatment.

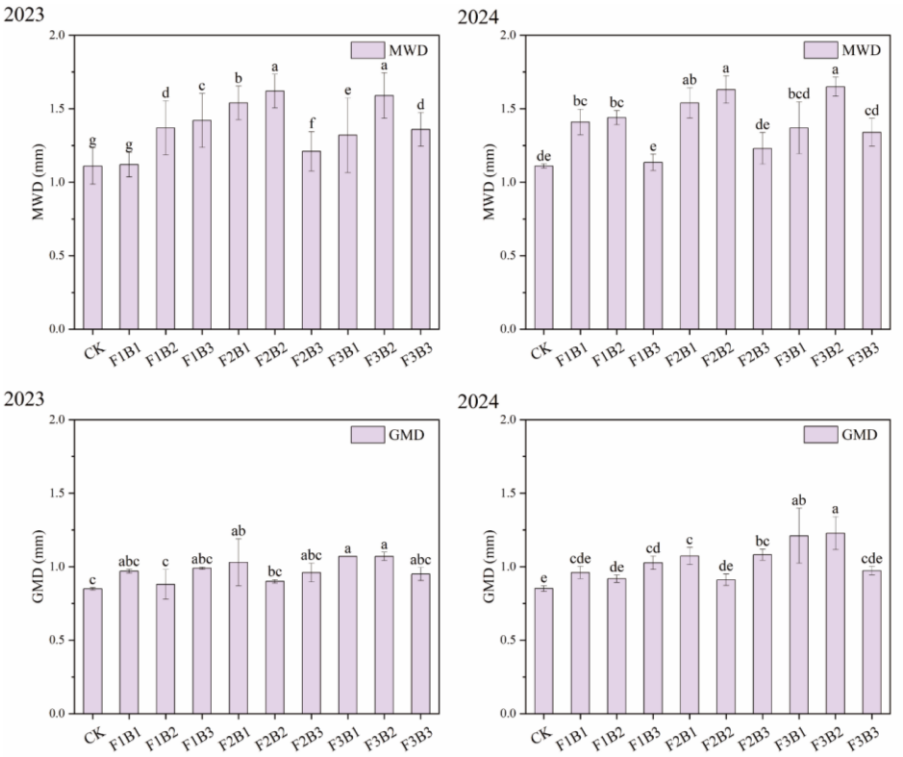

Figure 3: Soil water-stable aggregate stability indicators

Figure 4: Soil nutrient measurement indicators

Results and Analysis

Soil property responses

Aggregate stability

As shown in Figure 3, different fertilization treatments significantly affected the mean weight diameter (MWD) of soil aggregates (p<0.05). In 2023, MWD values across all treatment groups generally ranged between 1 and 1.5 mm, with higher MWD values observed under treatments F3B2 and F2B2. Among these, the unfertilized control (CK) exhibited the lowest MWD value at only 1.11 mm. Notably, the geometric mean diameter of aggregates showed a significant correlation with biochar application rate (p<0.05). As biochar application increased, the mean weight diameter (MWD) of soil aggregates exhibited a trend of first increasing and then decreasing. In the year 2024, MWD values slightly increased across all fertilized treatments, with the highest reaching 1.65 mm, indicating that fertilization measures effectively improved soil aggregate stability. Among these, F3B2 showed the most improvement. Its MWD value was about 0.06 mm higher than in 2023, which is a 3.77% increase. It performed significantly better than the other treatments. Next were F2B2 and F2B1. Their MWD values were 1.63 mm and 1.54 mm, respectively. They also demonstrated good improvement. Compared to the control group, it is clear that adding organic fertilizer and biochar under reduced nitrogen conditions enhanced aggregate stability. In the year 2023, the geometric mean diameter (GMD) of soil aggregates showed little variation across treatments, with the highest values recorded under treatments F3B1 and F3B2, both at 1.07 mm. Compared to 2023, the geometric mean diameter (GMD) of soil aggregates under the F3B2 treatment in 2024 increased by 14.95% over the previous year and showed significant differences from all other treatments (p<0.05).

Soil nutrient content

Throughout the experiment, the soil nutrient content exhibited a full-cycle pattern, as shown in Figure 4. Based on the combined results from two years, during the T1 period, nutrient levels in all treatments supplemented with organic fertilizer and biochar were lower than those in the control group treated with chemical fertilizer. As the growing season progressed, the variations in available potassium and available phosphorus content across treatments became more pronounced, while the fluctuations in total nitrogen content remained relatively smaller.

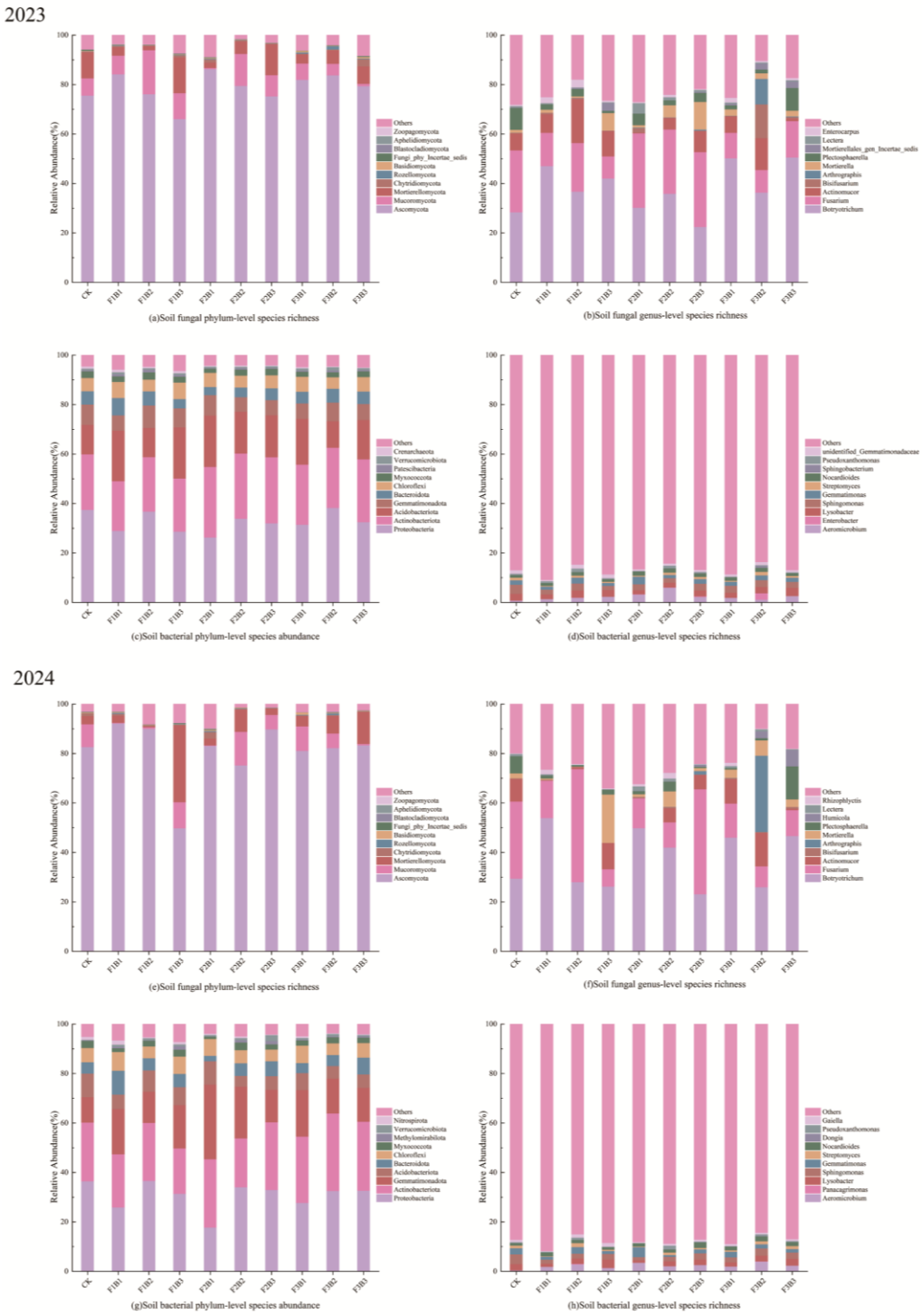

Figure 5: Relative abundance of species at the phylum and genus levels of soil fungi and bacteria

In the year 2023, under different organic fertilizer applications, the available potassium content in the T3 period also exhibited the same trend with biochar application rates, showing an initial increase followed by a decrease. Notably, during the T1 and T2 periods, the available potassium content reached higher levels in the F3B2 treatment. It can be observed that both available phosphorus and total nitrogen content gradually decreased as the growth stage progressed, with some treatments exhibiting a trend of first increasing and then decreasing. Analysis of soil total nitrogen revealed that treatments incorporating organic fertilizer exhibited higher total nitrogen levels than the control group during the T3 stage. Among the organic fertilizer treatments, the F3 treatment maintained relatively high soil total nitrogen levels throughout all growth stages. The F3B2 treatment reached its maximum total nitrogen content during the T3 stage, exceeding the control group by 1.04 g kg^{-1} during the same period.

In the year 2024, compared to 2023, the available potassium content in all treatments showed slight increases throughout the entire growth period. Overall, the available potassium content was lowest during the T2 stage. As time progressed, the content recovered in most treatments by the T3 stage. Among these, the available potassium content in both the F2B3 and F2B2 treatments exhibited a trend of first increasing and then decreasing. The F2B3 treatment reached its highest available potassium content at 424.92 mg kg^{-1} during the T2 stage. Available phosphorus content generally followed an increasing-then-decreasing trend, with a more pronounced decline during the T3 stage. The F2B2 treatment exhibited a 62.11% reduction in available phosphorus content during the T3 stage compared to the T2 stage. Compared to the year 2023, total nitrogen content showed smaller variations across all treatments in the year 2024. Overall, treatments incorporating organic fertilizer and biochar demonstrated increased total nitrogen content relative to the control group despite reduced nitrogen application rates.

Soil microecological response

Relative species abundance

Observation of Figure 5 reveals that the bacterial community composition ranked by relative abundance at the phylum level showed no significant differences among the top 10 phyla. However, under different treatment conditions, the abundance proportions of various bacterial phyla exhibited marked variations. The top 10 bacterial phyla by relative abundance in the soil revealed in Figure 5 indicate that *Proteobacteria* was the most species-rich phylum across all treatments. This phylum is extensively involved in soil carbon and nitrogen cycling processes. In 2023, its abundance peaked at 38.28% under treatment F3B2, while the lowest abundance was observed in the F2B1 treatment at 26.31%. *Actinobacteria*, a key contributor to soil secondary metabolites, ranked second in abundance. Its abundance peaked at 31.35% under the F2B3 treatment in 2024 and reached its lowest point at 18.37% under the F1B3 treatment. Bacteria belonging to the *Acidobacteria* phylum ranked third in abundance. Low-concentration biochar significantly increased the abundance of *Acidobacteria*, while the enhancement effects of high- and medium-concentration biochar were moderate. Comprehensive analysis of the top three bacterial phyla reveals that in 2024, the F3B2 treatment exhibited the highest overall abundance, while the F1B1 treatment showed the lowest. Additionally, compared to the year 2023, two new phyla—*Crenarchaeota* and *Patescibacteria*—emerged in the year 2024.

Analysis of the bacterial community structure at the genus level revealed that with increasing biochar application, the abundance of the top 10 bacterial genera under different organic fertilizer treatments first increased and then decreased (Figure 5). Among these, the top 10 bacterial genera under the F3B2 treatment reached their maximum total proportion in both 2023 and 2024, with total ratios of 16.37% and 15.70%, respectively. while the F1B1 treatment showed the lowest total proportions at 9.14% and 8.27%, respectively. *Aeromicrobium*, classified under the phylum *Actinobacteria*, was the most abundant genus in Figure 5. Its abundance peaked at 3.99% in the F2B2 treatment in 2024 and reached its lowest value of 0.44% in the control group (CK). Notably, *Enterobacter* was significantly present in the F3B2 treatment, reaching a ratio of 2.61% in 2023, but this genus was not clearly detected in other treatments. For the genus *Sphingobacterium*, bacterial abundance showed a significant increase in the F3B2 treatment, with abundance ratios of 0.82% in 2023 and 0.19% in 2024. However, this genus was not detected in the F1B1, F1B3, and F3B3 treatments.

Observation of Figure 5 reveals significant changes in fungal abundance at the phylum level across different fungal taxa. Among the top 10 soil fungal phyla by relative abundance depicted in Figure 5, *Ascomycota* was the most species-rich group across all treatments. Its abundance peaked at 86.29% under the F2B1 treatment in the year 2023 and reached its lowest point at 66.11% under the F1B3 treatment. *Mucoromycota* ranked second in abundance among soil fungal phyla. Compared to 2023, the abundance

of *Mucoromycota* in the F1B3 treatment decreased by 96.07% in 2024. *Mortierellomycota* ranked third in abundance. Analyzing data from both years, it exhibited the highest abundance in the F1B3 treatment at 14.49%, with its relative abundance increasing by 114.48% in the second year compared to the first. Additionally, the remaining seven phyla, in order of descending relative abundance, were (1) *Chytridiomycota*, (2) *Rozellomycota*, (3) *Basidiomycota*, (4) Fungi *incertae sedis* (unclassified at the phylum level), (5) *Blastocladiomycota*, (6) *Aphelidiomycota*, and (7) *Zoopagomycota*. All contribute extensively to the sustainable development of the soil microenvironment.

The overall abundance of the top 10 fungal genera under different organic fertilizer treatments showed an initial increase followed by a decrease with increasing biochar addition, as revealed by the genus-level community structure analysis (Figure 5). Notably, the total abundance of the top 10 fungal genera reached the highest proportions in the F3B2 treatment in both 2023 and 2024, accounting for 89.68% and 90.13%, respectively. *Botryotrichum* was the most abundant genus at the genus level in soil fungi. In 2024, its abundance peaked at 53.96% in the F1B1 treatment. As shown in Figure 5, the abundance of *Fusarium* was lower than that of the control group (CK) in most treatments. Specifically, its abundance in the F1B3 treatment in 2024 was only 7.03%, while the F1B2 treatment reached 45.71%. This indicates that excessive biochar significantly reduced *Fusarium* abundance. Additionally, compared to 2023, two new genera—*Rhizophlyctis* and *Humicola*—emerged in 2024.

Analysis of alpha diversity in soil microbial communities

The systematic statistical analysis of soil bacterial alpha diversity indices revealed that all treatments achieved Good's coverage values exceeding 99%, as shown in Table 4. Observation reveals that the Chao1 index for soil bacteria under treatment F3B2 achieved the maximum values of 3028.06 and 3087.18 in 2023 and 2024, respectively. Furthermore, while the Chao1 index showed no highly significant differences across most treatments in 2023, it exhibited significant differences ($p<0.05$) among treatments in 2024. Furthermore, in both 2023 and 2024, the F1B3 treatment yielded the lowest Chao1 indices for soil bacteria at 2353.65 and 2552.55, respectively, showing significant differences compared to most other treatments ($p<0.05$). In 2023, the Shannon index reached its maximum value of 10.396 under the F3B1 treatment, while the minimum value of 10.11 was observed under F1B3. Analysis of treatments revealed that under cattle manure (F2) and earthworm castings (F3) applications, biochar addition at different gradients did not significantly affect the Shannon index. In summary, earthworm castings (F3) were the most effective at increasing soil bacterial diversity. Specifically, while higher biochar rates reduced diversity under chicken manure (F1), earthworm castings (F3) with moderate biochar achieved the peak diversity value in 2024 (a 2.81% increase over the control), significantly outperforming both chicken manure (F1) and cattle manure (F2) treatments.

Analysis of soil fungal alpha diversity indices (Table 4) revealed systematic patterns, with the Chao1 index specifically reflecting fungal richness. The graph shows that fungal richness peaked at 590.31 in 2023 and 637.72 in 2024 under the F3B2 treatment, representing an 8.03% increase from the previous year. In the F1 treatment, soil fungal abundance exhibited a gradual decline with increasing biochar addition. Treatments F2 and F3 demonstrated nonlinear responses, showing an initial increase followed by a decrease in fungal abundance with biochar addition, peaking at the medium biochar dose (B2). Compared to the control group (CK), all other treatments increased the Shannon index, with the F3B2 treatment achieving the highest values of 5.18 and 5.63 in 2023 and 2024, respectively. It was observed that the Shannon index also showed an initial increase followed by a decrease with the gradual addition of biochar. Notably, the improvement effect in 2024 was more pronounced than in 2023, with all treatments showing greater increases compared to the previous year.

Beta diversity analysis of soil microbial communities

The analysis revealed that in 2023, PC1 and PC2 represented 25.72% and 16.54% of the total variance, respectively (Figure 6a). Together, these two axes cumulatively explained 42.27% of the community variation, reflecting the vast majority of differences among the samples. Figure 6a reveals that the overall sample community diversity is partitioned into three modules. One module clusters predominantly in the positive half of the PC2 axis with high aggregation, though F1B1 exhibits distinct differentiation within it. The second module concentrates on the negative half of PC2, primarily comprising treatments F1B3, F1B2, F2B2, and CK, though these four treatments are not closely clustered. F3B2 forms an independent cluster, indicating that species diversity under this treatment differs significantly from other treatments. In 2024, the PC1 axis contributed 25.46% of the total variance, while the PC2 axis contributed 15.29%,

together explaining 40.75% of the community variation (Figure 6b). Figure 6b reveals that the overall sample community diversity is partitioned into four modules. One cluster is concentrated in the positive half of the PC2 axis, indicating significant structural differences between the F1B1 and F2B1 communities. The second cluster, centered in the first quadrant, primarily includes treatments F1B3 and F2B2, exhibiting relatively consistent microbial community structures. The third cluster, also in the first quadrant, comprises treatments F1B3, CK, and F2B2, with CK and F2B2 showing similar microbial community structures. Treatment F1B2 forms an isolated cluster, indicating its species diversity differs significantly from the other treatments.

Table 4: Alpha diversity indices of soil fungi and bacteria in tomato rhizosphere

	2023						2024					
	viruses			fungi			viruses			fungi		
Treatment	Chao1	Shannon	Goods coverage (%)	Chao1	Shannon	Goods coverage (%)	Chao1	Shannon	Goods coverage (%)	Chao1	Shannon	Goods coverage (%)
CK	2749.60±184.47ab	10.143±0.0871bc	99.61%	425.12±21.37e	3.58±0.24c	99.99%	2605.32±125.72de	10.126±0.0042	99.61%	457.88±18.39f	3.65±0.11e	99.73%
F1B1	2805.54±170.13a	10.372±0.0369ab	99.56%	550.77±15.30abc	4.41±0.25abc	99.83%	2837.59±97.04c	10.241±0.0092	99.56%	561.62±7.88bc	4.67±0.10c	99.71%
F1B2	2431.32±118.97bc	10.112±0.1003c	99.67%	461.89±35.75de	4.64±0.11ab	99.70%	2747.23±105.54cd	10.119±0.0204	99.67%	489.51±22.39e	4.69±0.08c	99.94%
F1B3	2353.65±198.18c	10.111±0.1154c	99.62%	438.70±31.64de	4.53±0.22abc	99.79%	2552.55±111.84e	10.143±0.0631	99.62%	447.86±13.92f	4.69±0.01c	99.61%
F2B1	2700.20±242.74ab	10.156±0.1743bc	99.66%	488.24±31.34cde	4.04±0.51bc	99.78%	2893.16±54.52bc	10.168±0.0576	99.66%	507.15±21.44e	4.27±0.33d	99.56%
F2B2	2746.81±133.51ab	10.261±0.1059abc	99.55%	536.45±25.42abc	4.40±0.48abc	99.68%	2916.27±110.81bc	10.166±0.0485	99.55%	537.84±23.66cd	4.58±0.23c	99.97%
F2B3	2794.67±78.667a	10.129±0.0886c	99.69%	436.31±33.80de	3.52±0.50c	99.89%	2820.48±82.93c	10.106±0.0293	99.69%	453.24±12.11f	3.66±0.11e	99.89%
F3B1	2895.65±41.520a	10.396±0.0190a	99.67%	566.47±30.42ab	4.33±0.55abc	99.90%	3007.29±66.29ab	10.349±0.0862	99.67%	586.71±15.37b	5.29±0.24b	99.88%
F3B2	3028.06±110.19a	10.290±0.1145abc	99.73%	590.31±21.59a	5.18±0.43a	99.99%	3087.18±58.83a	10.411±0.0400	99.73%	637.72±5.85a	5.63±0.20a	99.90%
F3B3	2749.22±68.547ab	10.212±0.0689abc	99.71%	502.19±36.50bcd	4.28±0.64abc	99.89%	2798.89±36.06c	10.249±0.0265	99.71%	517.78±15.52de	4.69±0.11c	99.99%

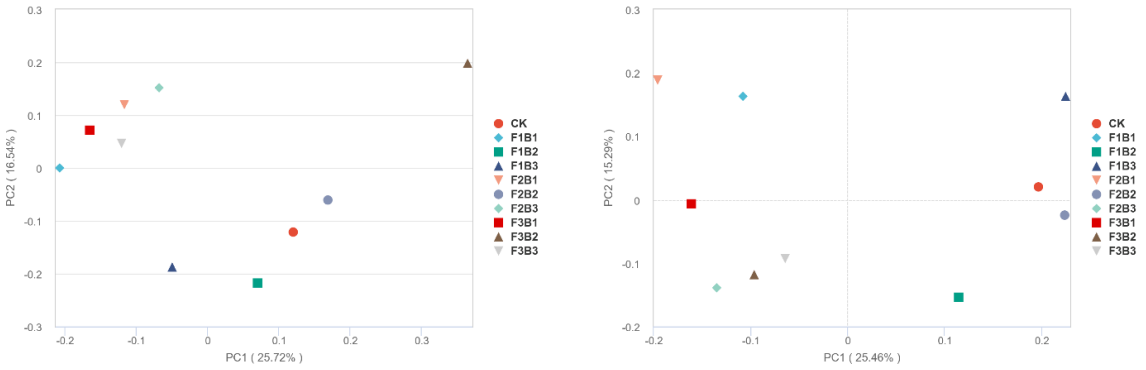

(a) PCoA analysis of soil bacteria (2023) (b) PCoA analysis of soil bacteria (2024)

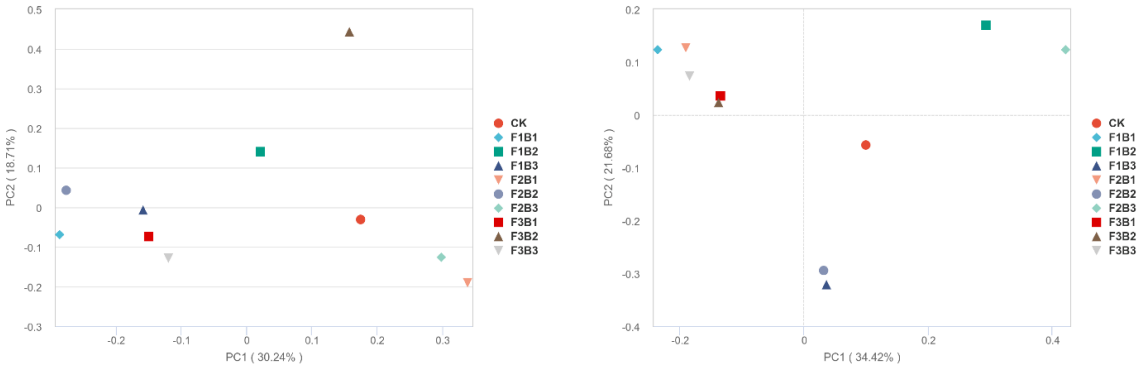

(c) PCoA analysis of Soil Fungi(2023) (d) PCoA analysis of Soil Fungi(2024)

Figure 6: PCoA analysis of bacteria and fungi

The principal component bivariate plot for fungi (Figure 6c) shows that in 2023, the variance explained by PC1 and PC2 was 30.24% and 18.71%, respectively. Together, they cumulatively accounted for 49.05% of community variability, reflecting the vast majority of differences among samples. The plot reveals that the overall sample community diversity is partitioned into three modules. One module clusters around the negative half-axis of PC2 with high aggregation, comprising F1B1, F1B3, F3B1, F3B3, and F2B2, though F2B2 exhibits distinct differentiation within this group. F1B3, F3B1, and F3B3 are the closest in proximity. The second cluster is concentrated on the positive half-axis of PC1, primarily comprising treatments CK, F2B3, and F2B1. CK maintains a certain distance from the other two treatments, indicating some diversity differences. F1B2 and F3B2 form an independent cluster, concentrated on the positive half-axes of both PC1 and PC2, with significant distance separation. In 2024, the PC1 axis accounted for 34.42% of the total variance, while the PC2 axis contributed 21.68%, collectively explaining 56.1% of the community variance (Figure 6d). Figure 6d reveals that the overall sample community diversity is partitioned into four modules. One module is concentrated in the positive half-axis region of PC2, exhibiting relatively minor differences in community structure. The second cluster is centered on the negative half-axis of PC2, primarily comprising treatments F3B3, F3B2, F2B3, and F3B1. Among these, F3B3, F3B2, and F2B3 exhibit relatively consistent microbial community structures. The third cluster is centered in the first quadrant of the coordinate system, primarily comprising treatments F1B2 and F1B1, though their microbial community structures exhibit some variation. The CK treatment forms a distinct cluster, indicating that the combined application of biochar and organic fertilizer alters fungal community structure.

Response of tomato yield and Quality

Production indicator

The average weight of tomato double-spike fruits was determined during the experiment (Figure 7). Observations reveal that in both 2023 and 2024, the F3B2 treatment yielded the highest average fruit weight for tomato double-spike fruit, increasing by 10.67% and 12.09%, respectively, compared to the control group CK ($p<0.05$). It was observed that under the F1 and F3 treatments, the average fruit weight of field-grown double-spike tomato fruits first increased and then decreased with increasing biochar application rates. Under the F2 treatment, the average fruit weight of field-grown double-spike tomato fruits gradually decreased with increasing biochar application rates. Notably, the F2B3 treatment yielded the lowest average fruit weight for field-grown tomato double-spike fruits in both years. Notably, the average fruit weight of field tomatoes' double-spike fruit in 2024 increased compared to the previous year.

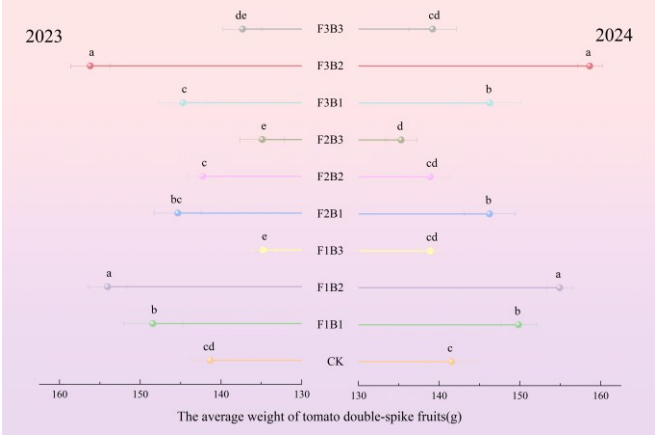

Figure 7: The average weight of tomato double-spike fruits under each treatment

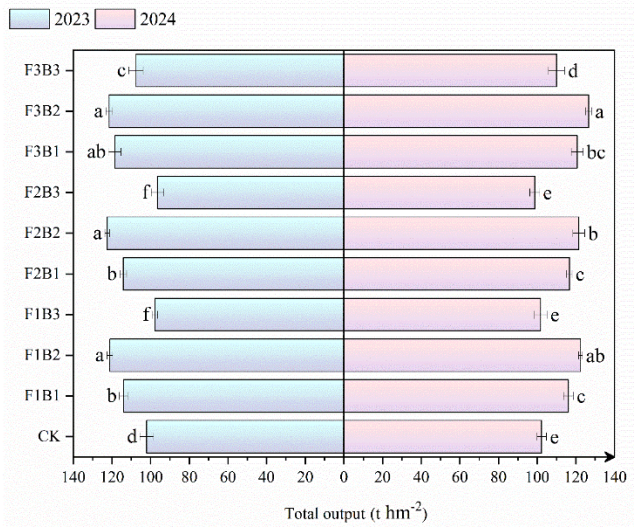

Figure 8: Total yield of tomatoes under each treatment

The total yield of field tomatoes was determined across the experiment, as illustrated in Figure 8. With increasing biochar application rates, total yield under different organic fertilizer treatments initially increased before declining. The maximum total fruit yield under various organic fertilizer conditions was achieved in the B2 treatment. When biochar was applied at the B2 rate, there was no significant difference in the positive effect of different organic fertilizers on total fruit yield. Notably, in 2023, the F2B2 treatment yielded the highest total field tomato

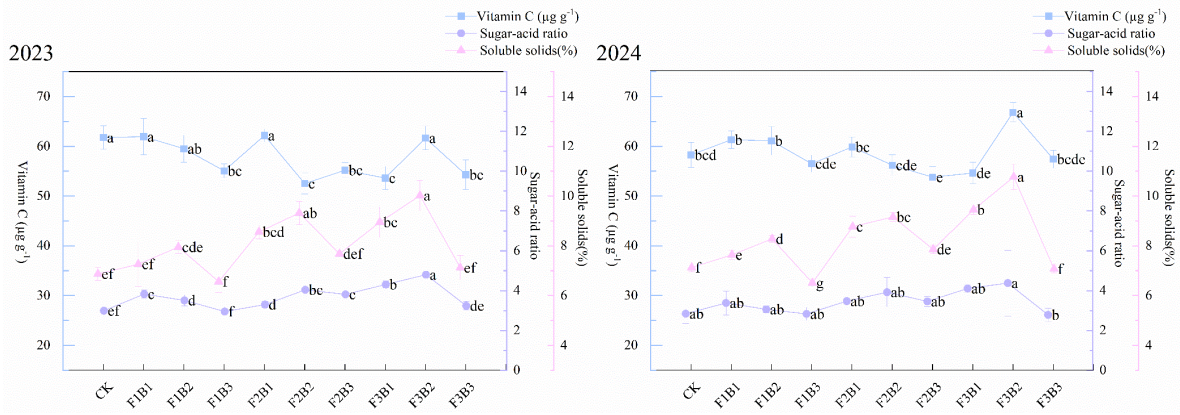

Figure 9: Quality indicators of tomato fruits under different treatments

Table 5: Relative proximity of soil traits, growth and yield quality of tomato roots to the ideal solution under each treatment

	2023				2024			
Treatment	Positive ideal solution distance D^+	Negative ideal solution distance D^-	Relative closeness C	Ranking results	Positive ideal solution distance D^+	Negative ideal solution distance D^-	Relative closeness C	Ranking results
CK	0.71432814	0.54750814	0.43389792	6	0.76246583	0.44042147	0.36613693	9
F1B1	0.70720774	0.48113953	0.40488125	7	0.71354752	0.43967429	0.38125735	7
F1B2	0.74124983	0.41583541	0.35938183	9	0.73025062	0.44924864	0.38088081	8
F1B3	0.8257525	0.33922469	0.2911857	10	0.92567717	0.11989642	0.11467048	10
F2B1	0.48013263	0.65412029	0.57669703	2	0.56070437	0.51956389	0.48095821	3
F2B2	0.64862436	0.57061414	0.46800863	5	0.60504189	0.53876069	0.47102594	4
F2B3	0.64018364	0.59266409	0.48072773	4	0.67135319	0.55664011	0.45329246	5
F3B1	0.59023813	0.5716968	0.49202135	3	0.48083519	0.64328518	0.57225649	2
F3B2	0.13155297	0.91440981	0.87422787	1	0.15796674	0.91787835	0.85316962	1
F3B3	0.71991021	0.45794901	0.38879775	8	0.67967954	0.45623265	0.4016443	6

production, representing a 19.58% increase compared to the control group (CK). The F2B3 treatment yielded the lowest total field tomato production, showing a 5.97% decrease relative to CK. For 2024, the top three treatments with the highest yields were F3B2, F1B2, and F2B2, with yields of 126.61 t hm^{-2}, 122.42 t hm^{-2}, and 121.55 t hm^{-2}, respectively, all showing increases compared to 2023.

Quality indicators

Significant differences in vitamin C content were observed among the treatments (Figure 9). In 2023, the F2B1 treatment yielded the highest vitamin C content at 62.17 μg g^{-1}, while the F2B2 treatment produced the lowest at 52.51 μg g^{-1}. Compared to the control group (CK), the vitamin C content in fruits under treatments F1B1, F2B1, and F3B2 showed no significant differences and ranked among the highest. Additionally, compared to the CK control, most treatments incorporating organic fertilizer exhibited a decrease in the growth rate of fruit vitamin C content. Among these, the F2B2 treatment showed the lowest value, with a growth rate reduction of 14.97% (p<0.05). In 2024, the F3B2 treatment achieved the highest value of 66.81 μg g^{-1}, representing a 7.46% increase compared to 2023 and showing significant differences from other treatments.

Under reduced nitrogen conditions, the coupled application of various organic fertilizers and biochar significantly positively influenced soluble solids content across most treatments. Compared to the control (CK), the F3B2 treatment showed the most pronounced increase, with soluble solids content rising by 49.64% in 2023 and 51.05% in 2024. While the F1B3 treatment exhibited the lowest soluble solids content, with growth rates decreasing by 4.45% and 8.70%, respectively (p<0.05). Comprehensive analysis of fruit sugar-acid ratios revealed that nitrogen reduction combined with organic fertilizer and biochar application partially enhanced fruit flavor intensity. In the F1 treatment, sugar-acid ratios gradually decreased with biochar addition. For F2 and F3 treatments, the sugar-acid ratio peaked under the B2 gradient of biochar. Specifically, in 2023, compared to CK, the F3B2 treatment achieved the highest increase in fruit sugar-acid ratio at 54.19%. Under F1B3 and F3B3 treatments, the increase in fruit sugar-acid ratio decreased by 0.05% and 1.84%, respectively. In 2024, the sugar-acid ratio increased compared to the previous year, but no significant differences were observed across treatments.

Comprehensive effect assessment of organic fertilizer coupled with biocharTOPSIS analysis was used to comprehensively evaluate how combined applications of organic fertilizers and biochar gradients affected nitrogen reduction, tomato rhizosphere soil properties, yield, and quality in field trials. The full results are shown in Table 5.

Observing the table reveals that, based on relative proximity to the ideal value, the top three treatments across both years were F3B2, F2B1, and F3B1, while the lowest-ranked treatment was F1B3. Comprehensive analysis further reveals that most treatments ranked higher than the control group, reaffirming that the coupled application of organic fertilizer and biochar comprehensively enhances tomato root zone soil properties, plant growth, and yield quality. Under the same organic fertilizer application treatment, the rankings for all biochar B3 application gradients declined. This further confirms that excessive biochar application in field trials can also negatively impact the comprehensive effects on root system soil properties, plant growth, and yield quality.

Discussion

Effects on soil physicochemical properties

Soil aggregates are the fundamental structural units of soil. Their content and particle size distribution not only influence crop growth and development but also significantly impact a series of physical, chemical, and biological processes in soil (Yudina & Kuzyakov, 2023). As shown in Figure 2, adding biochar markedly enhances soil aggregate stability, while organic fertilizer application significantly promotes aggregate formation, thereby further improving soil structure (Tian *et al.*, 2022). When the Mean Width Distribution (MWD) is significantly higher than the Granular Mean Diameter (GMD), it indicates that a small number of large aggregates dominate soil stability, while micro-aggregates exhibit greater dispersion; conversely, when the two are close, it reflects a more uniform particle size distribution. This study found that MWD was higher than GMD, indicating that large aggregates played a more dominant role. This may be because small stones may be present in field cultivation. However, the difference became more pronounced after adding organic fertilizer, demonstrating that organic fertilizer addition can further promote aggregate formation and improve soil structure (Rabot *et al.*, 2018). This study found that after organic fertilizer application, all agglomerate stability indicators improved to some extent, confirming that organic fertilizer addition further promotes agglomerate formation and improves soil structure. Wu *et al.* (2020) investigated the effects of increased organic fertilizer application and reduced chemical fertilizer use on grape root zone soil properties. Results indicated that increased organic fertilizer application enhanced sustainable soil productivity while elevating soil organic matter, available nitrogen, available phosphorus, and available potassium content in root zone soil. This partially aligns with the present study's findings, further confirming that organic fertilizer application regulates sustainable soil utilization. Lin *et al.* (2019) examined soil aggregate formation and organic matter content in soils amended with organic fertilizers. Findings revealed enhanced aggregate formation and a positive increase in organic matter content, aligning with the results of this study. Zhang *et al.* (2024) investigated the effects of reducing chemical nitrogen fertilizer and increasing organic and silicon fertilizers on plant growth in greenhouse tomatoes. Results indicated that this fertilization strategy increased soil organic matter, total nitrogen, and available nutrients, thereby significantly enhancing tomato fruit length, width, individual fruit weight, and yield. This aligns with some findings of the present study. Evidently, the addition of organic fertilizers or biochar facilitates soil aggregate formation, enhances aggregate stability, and increases soil nutrient content.

Regulatory mechanisms of soil microecosystems

Bacteria within soil microorganisms are central drivers of ecosystem function. By secreting hydrolytic enzymes and other substances, soil bacteria convert plant and animal residues into soluble nutrients, playing a crucial role in organic matter decomposition, nutrient cycling, and plant health maintenance (Aloo *et al.*, 2019). Certain bacteria can also convert atmospheric nitrogen into ammonia through biological nitrogen fixation, a process achieved either by free-living bacteria or those in symbiosis with plants. Statistics indicate these bacteria add over 100 megatons of nitrogen to global soils annually (Fowler *et al.*, 2013). Furthermore, research indicates that soil bacteria enhance plant uptake of nitrogen from the soil (Adesemoye *et al.*, 2010). Therefore, agricultural practices that optimize soil bacterial community diversity and abundance can ensure efficient nitrogen supply while reducing chemical fertilizer application. Existing research indicates that heavy chemical fertilizer application negatively impacts soil bacterial diversity, while combined application of organic and chemical fertilizers can enhance it (Cai *et al.*, 2017). This study similarly found that compared to the control group, the coupled application of organic fertilizer and biochar under reduced nitrogen conditions increased soil bacterial species diversity

and abundance. Liu *et al.* (2021) investigated changes in soil bacterial communities using rice as a model crop, comparing organic and inorganic fertilizer applications. Their results indicated that replacing inorganic fertilizers with organic fertilizers significantly altered soil bacterial community structure and increased relative bacterial abundance, consistent with some findings in this study. Ikoyi *et al.* (2020) found that compared to inorganic fertilizers, rye grass rhizosphere under cow manure fertilization exhibited significantly higher bacterial abundance, including various bacteria capable of supplying effective plant nutrients. Existing research has confirmed that biochar can influence soil microbial community structure by creating a more favorable environment for soil bacteria, thereby enhancing bacterial growth efficiency (Lehmann *et al.*, 2011). This study similarly observed that moderate biochar addition across different organic fertilizer treatments increased soil bacterial community diversity and abundance. This effect may arise because bacteria adsorb onto biochar surfaces, reducing their leaching from the soil and thereby increasing bacterial abundance (Pietikäinen *et al.*, 2000). The study also revealed that excessive biochar application can cause certain negative effects. This may be due to the potential toxicity of some active organic compounds and heavy metals present in biochar itself to soil microorganisms. Biochar adsorption and hydrolysis of signaling molecules can disrupt interspecies communication among microorganisms, potentially altering soil microbial community structure and causing adverse effects (Zhu *et al.*, 2017).

Fungi and soil microorganisms are key participants in ecosystem material cycles and plant interactions, extensively involved in organic matter decomposition, nutrient activation, and other processes. Rashid *et al.* (2016) demonstrated that fungi play a significant role in N_2 fixation in mildly and moderately degraded soils. They transfer carbon and phosphorus from plant roots to associated bacteria in exchange for N_2 fixation, directly participating in organic matter decomposition while simultaneously activating nutrients. Fungi also play a vital role in stabilizing soil structure by forming mycelium networks around soil particles to create microaggregates, thereby enhancing soil erosion resistance (Peng *et al.*, 2013). Furthermore, fungal community diversity and species abundance serve as biological indicators of soil health, influencing ecosystem stability (Yang *et al.*, 2018). Therefore, rationally analyzing the diversity and abundance of fungal communities in soil is crucial for sustainable agricultural development and healthy crop growth. Allison *et al.* (2007) found that nitrogen fertilizer application rates significantly influence soil fungal communities, with the Shannon index decreasing markedly with nitrogen fertilizer application. This indicates that excessive nitrogen fertilizer application can damage soil fungal community diversity. This study investigated the effects of applying biochar and organic fertilizer under reduced nitrogen conditions on soil fungal communities. Results revealed changes in fungal community structure across treatments, with the F3B2 treatment achieving the highest alpha diversity indices. This indicates enhanced diversity and abundance within fungal communities. Cao *et al.* (2024) similarly investigated the effects of coupled organic fertilizer and biochar application on soil fungi in rice systems. Their findings revealed significant impacts on fungal diversity and abundance, partially consistent with our results. Evidently, organic fertilizer application mitigates the detrimental effects of excessive nitrogen fertilizer on soil fungi. This may stem from the activation of certain fungal genera by organic treatment—microbial groups predominantly rare in unfertilized soils—while simultaneously enhancing fungal metabolic potential in lipid and vitamin pathways. This boosts microbial resilience against external contamination, further optimizing soil fungal communities (Yu *et al.*, 2024).

Furthermore, this study also observed positive responses in soil fungal communities to the coupled application of biochar. This is attributed to biochar creating a favorable microenvironment for fungal survival, with its pores providing habitats and significantly enriching fungal mycelium development (Jaafar *et al.*, 2014). Notably, certain saprophytic fungi may transform into plant pathogens. In this study, Fusarium (genus Fusarium) was detected, posing a risk of causing tomato wilt disease. However, except for the F2B3 treatment, fungal abundance remained lower than the control group in all other treatments. However, related studies also indicate that animal manure fertilizers may increase the abundance of viruses associated with human diseases and enrich pathogens and virulence factors in the soil, posing ecological risks. Therefore, their use requires analysis and testing (Yu *et al.*, 2024).

Synergistic effects on crop yield and Quality

During tomato plant growth, the rhizosphere soil microenvironment serves as a microscopic indicator of response, while yield represents a crucial measure of crop growth efficiency. This study found that applying organic fertilizer and biochar under reduced nitrogen conditions significantly boosted tomato plant yields. This effect likely stems from the substantial improvement in soil structure achieved through organic fertilizer application. Comprehensive soil nutrient analysis revealed that adding organic fertilizer and biochar enriched the soil nutrient pool, further facilitating smoother tomato plant growth. Velli *et al.* (2021) investigated tomato growth using organic fertilizer and biochar. Their findings revealed that biochar

addition significantly increased available nutrient content in the soil while also markedly enhancing tomato plant dry weight. Gu *et al.* (2025) investigated wheat growth under reduced nitrogen conditions through the combined application of organic fertilizer and biochar. Results indicated that the coupled application of biochar and organic fertilizer could reduce chemical fertilizer use while simultaneously increasing wheat yield, consistent with the yield enhancement observed for tomatoes in this study.

Tomato fruit quality assessment is a critical component of high-quality tomato cultivation, where both nutritional value and sensory attributes play vital roles. Vitamin C, soluble solids, soluble sugars, and total acidity serve as key indicators for evaluating tomato nutritional quality and flavor. This study found that moderate nitrogen reduction enhances vitamin C content in tomato fruits. This may occur because reduced nitrogen partially stimulates the plant's antioxidant synthesis mechanisms. Concurrently, biochar's water and nutrient retention properties, along with the diverse organic matter in organic fertilizers, further enhance the activity of nitrogen-regulating enzymes in the soil. Heeb *et al.* (2005) investigated the effects of different nitrogen forms on tomato yield, quality, and taste. They found that appropriately reducing nitrogen fertilizer increased vitamin C content in tomato fruits, which was related to nitrogen-regulated antioxidant enzyme activity. This aligns with some findings of the present study. García *et al.* (2019) demonstrated that soil humic acids elevate tomato vitamin C content by activating antioxidant enzymes like SOD and CAT, with particularly pronounced effects under nitrogen-limited conditions. Organic fertilizers are notably rich in humic acids. The accumulation of soluble solids and soluble sugars may benefit from biochar-enhanced rhizosphere environments promoting carbon metabolism, while the slow-release potassium from organic fertilizers strengthens sugar transport to the fruit (Agegnehu *et al.*, 2017). This study also found that applying organic fertilizer and biochar under reduced nitrogen regulation improved the sugar-acid ratio of tomatoes and enhanced their flavor and texture.

Conclusion

This study used tomatoes as the research subject, aiming to investigate the effects of applying organic fertilizer and biochar under reduced nitrogen conditions on the soil properties of tomato root systems, as well as on crop yield and quality improvement. Additionally, the study conducted further research and analysis on the microecological environment of root system soils in field cultivation conditions. The study conclusively demonstrated that under reduced nitrogen conditions, the application of biochar and organic fertilizer can enhance soil aggregate quality, formation, and stability and improve soil structure, and that moderate reduction of nitrogen fertilizer application can also promote soil aggregate stability, thereby optimizing soil nutrient reserves and achieving sustainable soil recycling. Additionally, the study revealed the central role of soil bacteria and fungi in ecosystem functions and found that the reasonable combination of organic fertilizer and biochar can enhance soil microbial diversity and richness. However, excessive biochar or nitrogen fertilizer may have negative effects. Furthermore, this novel fertilization system can significantly increase tomato yields and improve quality indicators such as vitamin C content and sugar-to-acid ratio in fruit.

Acknowledgments

The authors thank the Yunnan Talent Support Plan Project (grant No. KKRD202223049) for providing financial support to this project.

References

Adesemoye, A.O., H.A. Torbert and J.W. Kloepper. 2010. Increased plant uptake of nitrogen from 15N-depleted fertilizer using plant growth-promoting rhizobacteria. *Applied Soil Ecology* 46(1): 54–58.

Agegnehu, G., A.K. Srivastava and M.I. Bird. 2017. The role of biochar and biochar-compost in improving soil quality and crop performance: A review. *Applied Soil Ecology* 119(10): 156–170.

Akhtar, S.S., G. Li, M.N. Andersen and F. Liu. 2014. Biochar enhances yield and quality of tomato under reduced irrigation. *Agricultural Water Management* 138(5): 37–44.

Alam, S.M.K., P. Li and M. Fida. 2024. Groundwater nitrate pollution due to excessive use of N-fertilizers in rural areas of Bangladesh: Pollution status, health risk, source contribution, and future impacts. *Exposure and Health* 16(1): 159–182.

Allison, S.D., C.A. Hanson and K.K. Treseder. 2007. Nitrogen fertilization reduces diversity and alters community structure of active fungi in boreal ecosystems. *Soil Biology and Biochemistry* 39(8): 1878–1887.

Aloo, B.N., B.A. Makumba and E.R. Mbega. 2019. The potential of Bacilli rhizobacteria for sustainable crop production and environmental sustainability. *Microbiological Research* 219(2): 26–39.

Bai, S.H., N. Omidvar, M. Gallart, W. Kämper, I. Tahmasbian, M.B. Farrar, K. Singh, G. Zhou, B. Muqadass, C.-Y. Xu, R. Koech, Y. Li, T.T.N. Nguyen and L. van Zwieten. 2022. Combined effects of biochar and fertilizer applications on

yield: A review and meta-analysis. *Science of the Total Environment* 808(2): 152073.

Bremner, J.M. and C.S. Mulvaney. 1982. Nitrogen—Total. p. 595-624. In: *Methods of soil analysis: Part 2 Chemical and Microbiological Properties*. 2nd Ed. A.L. Page (ed.). American Society of Agronomy and Soil Science Society of America, Madison, WI.

Cai, F., G. Pang, R.-X. Li, R. Li, X.-L. Gu, Q.-R. Shen and W. Chen. 2017. Bioorganic fertilizer maintains a more stable soil microbiome than chemical fertilizer for monocropping. *Biology and Fertility of Soils* 53(8): 861–872.

Cao, X., J. Liu, L. Zhang, W. Mao, M. Li, H. Wang and W. Sun. 2024. Response of soil microbial ecological functions and biological characteristics to organic fertilizer combined with biochar in dry direct-seeded paddy fields. *Science of the Total Environment* 948(10): 174844.

Cheng, Y., G. Xu, X. Wang, P. Li, X. Dang, W. Jiang, T. Ma, B. Wang, F. Gu and Z. Li. 2023. Contribution of soil aggregate particle size to organic carbon and the effect of land use on its distribution in a typical small watershed on Loess Plateau, China. *Ecological Indicators* 155(11): 110988.

Di Bella, J.M., Y. Bao, G.B. Gloor, J.P. Burton and G. Reid. 2013. High throughput sequencing methods and analysis for microbiome research. *Journal of Microbiological Methods* 95(3): 401–414.

Fowler, D., M. Coyle, U. Skiba, M.A. Sutton, J.N. Cape, S. Reis, L.J. Sheppard, A. Jenkins, B. Grizzetti, J.N. Galloway, P. Vitousek, A. Leach, A.F. Bouwman, K. Butterbach-Bahl, F. Dentener, D. Stevenson, M. Amann and M. Voss. 2013. The global nitrogen cycle in the twenty-first century. *Philosophical Transactions of the Royal Society B: Biological Sciences* 368(1621): 20130164.

García, A.C., T.A. van Tol de Castro, L.A. Santos, O.C.H. Tavares, R.N. Castro, R.L.L. Berbara and J.M. García-Mina. 2019. Structure–property–function relationship of humic substances in modulating the root growth of plants: A review. *Journal of Environmental Quality* 48(6): 1622–1632.

Gu, K., K. Gao, S. Guan, J. Zhao, L. Yang, M. Liu and J. Su. 2025. The impact of the combined application of biochar and organic fertilizer on the growth and nutrient distribution in wheat under reduced chemical fertilizer conditions. *Scientific Reports* 15(1): 5285.

Heeb, A., B. Lundegårdh, T. Ericsson and G.P. Savage. 2005. Nitrogen form affects yield and taste of tomatoes. *Journal of the Science of Food and Agriculture* 85(8): 1405–1414.

Hong, Y., D. Li, C. Xie, X. Zheng, J. Yin, Z. Li, K. Zhang, Y. Jiao, B. Wang, Y. Hu and Z. Zhu. 2022. Combined apatite, biochar, and organic fertilizer application for heavy metal co-contaminated soil remediation reduces heavy metal transport and alters soil microbial community structure. *Science of the Total Environment* 851(12): 158033.

Hu, W., Y. Zhang, X. Rong, X. Zhou, J. Fei, J. Peng and G. Luo. 2024. Biochar and organic fertilizer applications enhance soil functional microbial abundance and agroecosystem multifunctionality. *Biochar* 6(1): 3.

Hu, W., Y. Zhang, R. Xiangmin, J. Fei, J. Peng and G. Luo. 2023. Coupling amendment of biochar and organic fertilizers increases maize yield and phosphorus uptake by regulating soil phosphatase activity and phosphorus-acquiring microbiota. *Agriculture, Ecosystems & Environment* 355(10): 108582.

Hu, X., J. Chen and L. Zhu. 2020. Soil aggregate size distribution and stability of farmland as affected by dry and wet sieving methods. *Zemdirbyste-Agriculture* 107(2): 179–184.

Ikoyi, I., B. Egeter, C. Chaves, M. Ahmed, A. Fowler and A. Schmalenberger. 2020. Responses of soil microbiota and nematodes to application of organic and inorganic fertilizers in grassland columns. *Biology and Fertility of Soils* 56(5): 647–662.

Jaafar, N.M., P.L. Clode and L.K. Abbott. 2014. Microscopy observations of habitable space in biochar for colonization by fungal hyphae from soil. *Journal of Integrative Agriculture* 13(3): 483–490.

Knudsen, D., G.A. Peterson and P.F. Pratt. 1982. Lithium, Sodium, and Potassium. p. 225-246. In: *Methods of Soil Analysis: Part 2 Chemical and Microbiological Properties*. 2nd Ed. A.L. Page (ed.). American Society of Agronomy and Soil Science Society of America, Madison, WI.

Lehmann, J., D.A. Bossio, I. Kögel-Knabner and M.C. Rillig. 2020. The concept and future prospects of soil health. *Nature Reviews Earth & Environment* 1(10): 544–553.

Lehmann, J., M.C. Rillig, J. Thies, C.A. Masiello, W.C. Hockaday and D. Crowley. 2011. Biochar effects on soil biota – A review. *Soil Biology and Biochemistry* 43(9): 1812–1836.

Lin, Y., G. Ye, Y. Kuzyakov, D. Liu, J. Fan and W. Ding. 2019. Long-term manure application increases soil organic matter and aggregation, and alters microbial community structure and keystone taxa. *Soil Biology and Biochemistry* 134(7): 187–196.

Liu, J., A. Shu, W. Song, W. Shi, M. Li, W. Zhang, Z. Li, G. Liu, F. Yuan, S. Zhang, Z. Liu and Z. Gao. 2021. Long-term organic fertilizer substitution increases rice yield by improving soil properties and regulating soil bacteria. *Geoderma* 404(12): 115287.

Miao, C.Q., Z.W. Cai, R. Zheng, J. Bai, J. Wang, T.H. Wang and X.Q.Wang. 2022. A study on optimal irrigation of

seed corn in Hexi based on entropy method, AHP and TOPSIS model. *Hubei Agricultural Sciences* 61(16): 12-17.

Olsen, S.R., C.V. Cole, F.S. Watanabe and L.A. Dean. 1954. Estimation of available phosphorus in soils by extraction with sodium bicarbonate. U.S. Dept. of Agriculture Circular No. 939. U.S. Dept. of Agriculture, Washington, D.C. 19 p.

Peng, S., T. Guo and G. Liu. 2013. The effects of arbuscular mycorrhizal hyphal networks on soil aggregations of purple soil in southwest China. *Soil Biology and Biochemistry* 57(2): 411–417.

Pietikäinen, J., O. Kiikkilä and H. Fritze. 2000. Charcoal as a habitat for microbes and its effect on the microbial community of the underlying humus. *Oikos* 89(2): 231–242.

Rabot, E., M. Wiesmeier, S. Schlüter and H.-J. Vogel. 2018. Soil structure as an indicator of soil functions: A review. *Geoderma* 314(3): 122–137.

Rashid, M.I., L.H. Mujawar, T. Shahzad, T. Almeelbi, I.M.I. Ismail and M. Oves. 2016. Bacteria and fungi can contribute to nutrients bioavailability and aggregate formation in degraded soils. *Microbiological Research* 183: 26–41.

Richardson, K., W. Steffen, W. Lucht, J. Bendtsen, S.E. Cornell, J.F. Donges, M. Drüke, I. Fetzer, G. Bala, W. von Bloh, G. Feulner, S. Fiedler, D. Gerten, T. Gleeson, M. Hofmann, W. Huiskamp, M. Kummu, C. Mohan, D. Nogués-Bravo, S. Petri , M. Porkka, S. Rahmstorf, S. Schaphoff, K. Thonicke , A. Tobian, V. Virkki, L. Wang-Erlandsson, L. Weber and J. Rockström. 2023. Earth beyond six of nine planetary boundaries. *Science Advances* 9(37): eadh2458.

Rivelli, A.R. and A. Libutti. 2022. Effect of biochar and inorganic or organic fertilizer co-application on soil properties, plant growth and nutrient content in Swiss Chard. *Agronomy* 12(9): 2089.

Rockström, J., O. Edenhofer, J. Gaertner and F. DeClerck. 2020. Planet-proofing the global food system. *Nature Food* 1(1): 3–5.

Saha, B., A. Fatima, S. Saha, S.K. Sahoo and P. Poddar. 2024. Environmental pollution due to improper use of chemical fertilizers and their remediation. p. 203-219. In: *Environmental contaminants*. P. Ganguly, J. Mandal, M. Paramsivam and S. Patra (eds.). Apple Academic Press Inc., Palm Bay, FL.

Tao, L., F. Li, C. Liu, X. Feng, L. Gu, B. Wang, S. Wen and M. Xu. 2019. Mitigation of soil acidification through changes in soil mineralogy due to long-term fertilization in southern China. *CATENA* 174(3): 227–234.

Tian, S., B. Zhu, R. Yin, M. Wang, Y. Jiang, C. Zhang, D. Li, X. Chen, P. Kardol and M. Liu. 2022. Organic fertilization promotes crop productivity through changes in soil aggregation. *Soil Biology and Biochemistry* 165(2): 108533.

Velli, P., I. Manolikaki and E. Diamadopoulos. 2021. Effect of biochar produced from sewage sludge on tomato (*Solanum lycopersicum* L.) growth, soil chemical properties and heavy metal concentrations. *Journal of Environmental Management* 297(11): 113325.

Wang, X., X. Wang, H. Sheng, X. Wang, H. Zhao and K. Feng. 2022. Excessive nitrogen fertilizer application causes rapid degradation of greenhouse soil in China. *Polish Journal of Environmental Studies* 31(2): 1527–1534.

Wu, L., Y. Jiang, F. Zhao, X. He, H. Liu and K. Yu. 2020. Increased organic fertilizer application and reduced chemical fertilizer application affect the soil properties and bacterial communities of grape rhizosphere soil. *Scientific Reports* 10(1): 9568.

Yang, G., C. Wagg, S.D. Veresoglou, S. Hempel and M.C. Rillig. 2018. How soil biota drive ecosystem stability. *Trends in Plant Science* 23(12): 1057–1067.

Yu, Y., Q. Zhang, J. Kang, N. Xu, Z. Zhang, Y. Deng, M. Gillings, T. Lu and H. Qian. 2024. Effects of organic fertilizers on plant growth and the rhizosphere microbiome. *Applied and Environmental Microbiology* 90(2): e0171923.

Yudina, A. and Y. Kuzyakov. 2023. Dual nature of soil structure: The unity of aggregates and pores. *Geoderma* 434(6): 116478.

Zhang, F., Y. Liu, Y. Liang, Z. Dai, Y. Zhao, Y. Shi, J. Gao, L. Hou, Y. Zhang and G.J. Ahammed. 2024. Improving the yield and quality of tomato by using organic fertilizer and silicon compared to reducing chemical nitrogen fertilization. *Agronomy* 14(5): 966.

Zhu, X., B. Chen, L. Zhu and B. Xing. 2017. Effects and mechanisms of biochar-microbe interactions in soil improvement and pollution remediation: A review. *Environmental Pollution* 227(8): 98–115.